

# Matrix Product State

*Academic project report*

## Quantum Computation and Quantum Information

*by*

**Abhishek**

Roll No: 1911007



**School of Physical Sciences**

**National Institute of Science Education and Research**

**Bhubaneswar**

**May 9, 2024**

## ABSTRACT

This report presents a concise overview of Matrix Product States (MPS) and Tensor Networks within the context of quantum physics. It covers the fundamental principles of MPS, including its representation and its significance in describing quantum many-body systems. The report also explores the concept of entanglement and its connection to MPS. Additionally, it discusses the concept of Singular Value Decomposition (SVD) and the Density Matrix Renormalization Group (DMRG), particularly in the context of MPS. Finally, the report concludes by solving the 1D Ising model and computing magnetization and correlation length.

# Contents

<b>1</b>	<b>Matrix Product State</b>	<b>1</b>
1.1	Importance of Matrix Product States (MPS) and Tensor Networks . .	1
1.2	A Basic introduction to Quantum Mechanics . . . . .	2
1.3	Matrix Product State . . . . .	4
1.3.1	An Example of MPS . . . . .	5
1.4	Tensor Networks . . . . .	6
1.5	Area Law . . . . .	6
1.6	Graphical Representation of MPS . . . . .	8
1.7	Singular Value Decomposition (SVD) . . . . .	8
1.7.1	Low-Rank Approximation . . . . .	8
1.7.2	Image Compression using SVD . . . . .	9
<b>2</b>	<b>Density Matrix Renormalization Group Algorithm (DMRG)</b>	<b>11</b>
2.1	Introduction . . . . .	11
2.2	DMRG in the MPS formulation . . . . .	12
2.3	iDMRG . . . . .	13
2.4	DMRG Algorithm . . . . .	13
<b>3</b>	<b>Transverse Field Ising Model (TFIM)</b>	<b>15</b>
3.0.1	Ordered Phase . . . . .	15
3.0.2	Disordered Phase . . . . .	16
3.0.3	Gapless Phase . . . . .	16
3.1	Results . . . . .	16

3.1.1	Correlation Length . . . . .	16
3.1.2	Magnetisation in x-axis . . . . .	17
3.1.3	Magnetisation in z-axis . . . . .	17
3.1.4	Max Bond Dimension $\chi$ . . . . .	18
<b>Appendix A</b>		<b>20</b>
3.1	Singular Value Decomposition (SVD) . . . . .	20

# List of Figures

1.1	(a) 4-site MPS with open boundary conditions; (b) 4-site MPS with periodic boundary conditions. . . . .	6
1.2	1D entanglement entropy . . . . .	7
1.3	A tensor $T$ with six indices . . . . .	8
1.4	Image compression using SVD . . . . .	10
1.5	Singular values in descending order. . . . .	10
2.1	DMRG graphical representation . . . . .	12
3.1	Correlation length vs $g$ for various lattice sizes . . . . .	17
3.2	$\langle \sigma^x \rangle$ vs $g$ for various lattice sizes. . . . .	17
3.3	$\langle \sigma^z \rangle$ vs $g$ for various lattice sizes. . . . .	18
3.4	Max bond dimension vs $g$ for various lattice sizes. . . . .	19

# List of Tables

# Chapter 1

## Matrix Product State

### 1.1 Importance of Matrix Product States (MPS) and Tensor Networks

This chapter presents a brief introduction to Matrix Product States (MPS). Quantum many-body systems, especially strongly correlated systems in condensed matter physics, hold immense significance in modern physics. They encompass various intriguing phenomena like spin glasses [1], frustrated magnets, and superconductors. However, their complexity arises from the many interacting components, making analytical and numerical solutions challenging. The Hilbert space dimension expands exponentially with the number of particles, except for integrable systems, where analytical solutions are feasible due to a symplectic manifold's differential systems and an equal number of constants of motion.

Yet, most of these models aren't integrable, requiring numerical treatments. Due to computational limitations, only small systems could be analyzed using brute-force diagonalization methods. Thankfully, many physical systems can be adequately described by focusing on local interactions, which confine crucial ground states to a small portion of the Hilbert space.

For such systems, the Matrix Product State (MPS) formalism emerges as a powerful variational approach to reconstruct ground states efficiently at zero temperature. It effectively parametrizes a more compact submanifold of the Hilbert space, focusing

on sectors with reduced entanglement between the system's components. The primary interest lies in low-energy states with minimal entanglement, which are crucial for understanding physical systems.

Ground and thermal states of Hamiltonians with local interactions follow the area law for entanglement, connecting low-energy states to those with low entanglement. The recent surge in interest in MPS stems from the density matrix renormalization group (DMRG) method developed by S. White et al. in the 1990s.

This report aims to introduce tensor networks and the reformulated DMRG within the MPS formalism from a quantum information perspective. A DMRG program will be implemented and tested for the Ising and bilinear-biquadratic (BLBQ) Heisenberg models [2], comparing numerical results to analytical solutions wherever possible.

## 1.2 A Basic introduction to Quantum Mechanics

This section is mostly taken from the thesis [3]. In the realm of quantum mechanics, the wave function  $|\psi\rangle \in H$  encapsulates the system's information. Here,  $H$  denotes the Hilbert space and  $|\psi\rangle$  is a vector with coefficients in the complex field. A two-level system (such as a spin-1/2 system) serves as an illustrative example:

$$|\psi\rangle = \alpha|\uparrow\rangle + \beta|\downarrow\rangle$$

where  $\{|\uparrow\rangle, |\downarrow\rangle\}$  forms a basis for  $H \subseteq \mathbb{C}^2$ . This vector is referred to as a ket. A corresponding bra is defined as  $\langle\psi| = \alpha^*\langle\uparrow| + \beta^*\langle\downarrow|$ . If we define  $|\uparrow\rangle \equiv |0\rangle$  and  $|\downarrow\rangle \equiv |1\rangle$ , the two-level system becomes a quantum bit (qubit), and the state  $|\psi\rangle = \alpha|0\rangle + \beta|1\rangle$  is a superposition of 0 and 1.

The scalar product of two states is given by:



$$|\psi\rangle = \alpha|0\rangle + \beta|1\rangle, \quad |\phi\rangle = \tilde{\alpha}|0\rangle + \tilde{\beta}|1\rangle \Rightarrow \langle\phi|\psi\rangle = \tilde{\alpha}^*\alpha + \tilde{\beta}^*\beta$$

Physical states are normalized such that  $\langle\psi|\psi\rangle = |\alpha|^2 + |\beta|^2 = 1$ . For a quantum state  $|x\rangle$ , the probability  $P$  of the system  $|\psi\rangle$  being in the state  $|x\rangle$  is given by  $P(|x\rangle) = |\langle x|\psi\rangle|^2$ . Upon measuring a defined state, the entire system undergoes a collapse, for instance:

$$|\psi\rangle = \alpha|0\rangle + \beta|1\rangle \xrightarrow{\text{measuring } \sigma_z} +1 \Leftrightarrow |\psi\rangle = |0\rangle$$

A collapse is a non-unitary operation. Apart from measurements, physical operations are represented by unitary operators, where  $U$  is unitary if and only if  $UU^\dagger = U^\dagger U = 1$ , and  $U^\dagger$  is the conjugate transpose of  $U$ .

The Pauli matrices serve as a prime example of unitary operators:

$$\sigma_x = \begin{pmatrix} 0 & 1 \\ 1 & 0 \end{pmatrix}, \quad \sigma_y = \begin{pmatrix} 0 & -i \\ i & 0 \end{pmatrix}, \quad \sigma_z = \begin{pmatrix} 1 & 0 \\ 0 & -1 \end{pmatrix} \quad (2.5)$$

These matrices possess the following characteristics:

$$\{\sigma_i, \sigma_j\} = 2\delta_{ij}, \quad [\sigma_i, \sigma_j] = 2i \sum_{k=1}^3 \epsilon_{ijk} \sigma_k \quad (2.6)$$

Unitary operations maintain the norm of a state. For  $|\psi'\rangle = U|\psi\rangle$ ,

$$\langle\psi'|\psi'\rangle = \langle U\psi|U\psi\rangle = \langle\psi|U^\dagger U|\psi\rangle = \langle\psi|\psi\rangle \quad (2.7)$$

This implies that the probability is always conserved ( $\sum P_i = 1$ ). Composite systems are represented by tensor products of Hilbert spaces:

$$|\psi_1\rangle \in H_1, \quad |\psi_2\rangle \in H_2, \quad \text{composite system} \quad |\psi_3\rangle \in H_3 = H_1 \otimes H_2 \quad (2.8)$$

In terms of basis states, for instance, qubits:

$$\{|0\rangle_1, |1\rangle_1\} \in H_1, \quad \{|0\rangle_1 \otimes |0\rangle_2, |1\rangle_1 \otimes |1\rangle_2, |0\rangle_1 \otimes |1\rangle_2, |1\rangle_1 \otimes |0\rangle_2\} \in H_3,$$

$$\{|0\rangle_2, |1\rangle_2\} \in H_2, \quad \dim(H_1) = \dim(H_2) = 2, \quad \dim(H_3) = \dim(H_1) \cdot \dim(H_2) = 4 \quad (2.9)$$

Hence, some potential states for  $|\psi_3\rangle$  are:

$$|\psi_3\rangle = \begin{cases} |0\rangle_1 \otimes |1\rangle_2, \\ \frac{1}{\sqrt{2}}(|0\rangle_1 \otimes |0\rangle_2 + |0\rangle_1 \otimes |1\rangle_2) \equiv |0\rangle_1 |+\rangle_2, \quad |+\rangle = \frac{1}{\sqrt{2}}(|0\rangle + |1\rangle), \\ \frac{1}{2}(|0\rangle_1 \otimes |0\rangle_2 - |0\rangle_1 \otimes |1\rangle_2 - |1\rangle_1 \otimes |0\rangle_2 + |1\rangle_1 \otimes |1\rangle_2), \\ \frac{1}{\sqrt{2}}(|0\rangle_1 \otimes |0\rangle_2 + |1\rangle_1 \otimes |1\rangle_2). \end{cases} \quad (2.10)$$

A system is termed entangled if a state is not represented by a product of states of the corresponding subsystems. Otherwise, it is called separable.

$$|\psi\rangle \in H_1 \otimes H_2 \text{ is entangled if and only if } \nexists |\psi_i\rangle \in H_i \text{ such that } |\psi\rangle = |\psi_1\rangle \otimes |\psi_2\rangle \quad (2.11)$$

Examples of separable and entangled states are:

$$|\psi\rangle = \begin{cases} |0, 0\rangle \rightarrow \text{separable}, \\ \frac{1}{2}(|0, 0\rangle + |0, 1\rangle + |1, 0\rangle + |1, 1\rangle) = |+, +\rangle \rightarrow \text{separable}, \\ \frac{1}{\sqrt{2}}(|0, 0\rangle + |1, 1\rangle) \equiv |\Phi^+\rangle \rightarrow \text{entangled}, \\ \frac{1}{\sqrt{2}}(|1, 0\rangle - |0, 1\rangle) \equiv |\Psi^-\rangle \rightarrow \text{entangled}. \end{cases}$$

## 1.3 Matrix Product State

A Matrix product state (MPS) is a representation [4] of a quantum state of many particles (across  $N$  sites), expressed as:

$$|\Psi\rangle = \sum_{\{s\}} \text{Tr} \left[ A_1^{(s_1)} A_2^{(s_2)} \dots A_N^{(s_N)} \right] |s_1 s_2 \dots s_N\rangle$$

where  $A_i^{(s_i)}$  are complex, square matrices of order  $\chi$  (known as the local dimension). Indices  $s_i$  iterate over states in the computational basis. For qubits,  $s_i \in \{0, 1\}$  and for qudits (d-level systems),  $s_i \in \{0, 1, \dots, d-1\}$ .

MPS is particularly useful for dealing with ground states of one-dimensional quantum spin models (e.g., the Heisenberg model). The parameter  $\chi$  is related to the entanglement between particles. If the state is a product state (i.e., not entangled), it can be described as an MPS with  $\chi = 1$ .

For translationally symmetric states, we can choose:

$$A_1^{(s)} = A_2^{(s)} = \dots = A_N^{(s)} \equiv A^{(s)}$$

In general, every state can be written in the MPS form (with  $\chi$  growing exponentially with the particle number  $N$ ). However, MPS are practical when  $\chi$  is small – for example, does not depend on the particle number. Except for a small number of specific cases (some mentioned in the section Examples), such a thing is not possible, though in many cases it serves as a good approximation.

The MPS decomposition is not unique. There are several introductions and resources available for further understanding. In the context of finite automata, MPS has been discussed extensively. Emphasis has also been placed on the graphical reasoning of tensor networks in various studies.

### 1.3.1 An Example of MPS

MPS are TN states that correspond to a one-dimensional array of tensors, such as the ones in Fig.2.1 In a MPS there is one tensor per site in the many-body system.

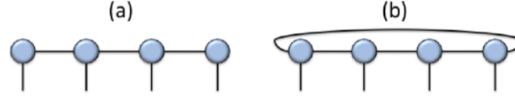


Figure 1.1: (a) 4-site MPS with open boundary conditions; (b) 4-site MPS with periodic boundary conditions.

The connecting bond indices that glue the tensors together can take up to  $D$  values, and the open indices correspond to the physical degrees of freedom of the local Hilbert spaces which can take up to  $p$  values.

## 1.4 Tensor Networks

Tensor network methods are taking a central role in modern quantum physics and beyond. During the last two decades, tensor networks have emerged as a powerful new language for encoding the wave functions of quantum many-body states, and the operators acting on them, in terms of contractions of tensors.

Insights from quantum information theory have led to highly efficient and accurate tensor network representations for a variety of situations, particularly for one- and two-dimensional (1d, 2d) systems.

## 1.5 Area Law

The Area Law states that for any ground state of local noncritical Hamiltonians, the entanglement entropy of a bipartition into regions A and B scales as the boundary of one of the two regions:

$$S(\rho_A) \propto \partial A \tag{1.5}$$

This has been verified for gapped systems in 1D. However, at Quantum criticality, logarithmic corrections may arise, especially for gapless Hamiltonians.

The Area Law can be visualized as the number of bonds required in the divide the system into 2 parts. For 1D, we can just cut the chain at any site, independent of length. For 2D, we have to cut the bonds across a line and the number of bonds we cut is proportional to the length of that line, hence it grows linearly. For 3D, we have to sweep across a surface and the number of bonds we cut is proportional to the area of that surface.

This has been contrasted with the volume law for entanglement entropy, which typically occurs for random states or for thermal states in non-equilibrium states. An interesting situation occurs in 1D, where the area-law condition means that the entropy does not scale at all with the size of the region  $A$ .

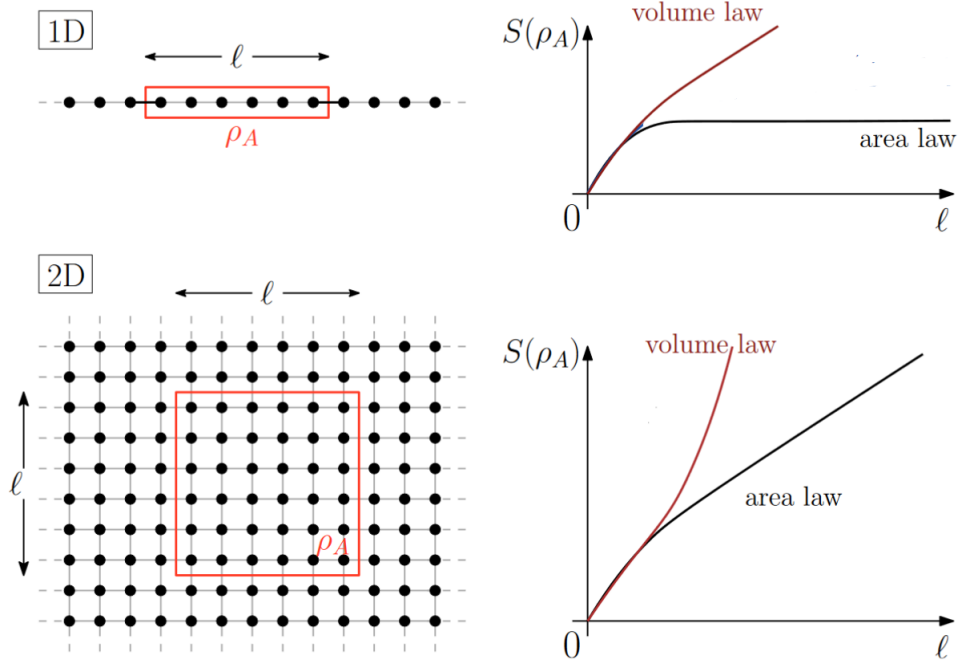


Figure 1.2: In 1D, the entanglement entropy doesn't scale with the size of the region. [5]

## 1.6 Graphical Representation of MPS

A matrix product state factorization of a tensor  $T$  can be expressed in tensor diagram notation [6] as:

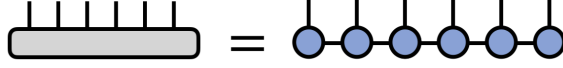


Figure 1.3: A tensor  $T$  with six indices

In traditional tensor notation, the same can be written as:

$$T^{s_1 s_2 s_3 s_4 s_5 s_6} = \sum_{\{\alpha\}} A_{\alpha_1}^{s_1} A_{\alpha_1 \alpha_2}^{s_2} A_{\alpha_2 \alpha_3}^{s_3} A_{\alpha_3 \alpha_4}^{s_4} A_{\alpha_4 \alpha_5}^{s_5} A_{\alpha_5}^{s_6} \quad (1.1)$$

where the bond indices  $\alpha$  are contracted.

## 1.7 Singular Value Decomposition (SVD)

The singular value decomposition (SVD) is a factorization of a matrix  $A$  into three matrices  $U$ ,  $\Sigma$ , and  $V$  such that:

$$A = U \Sigma V^\dagger \quad (1.2)$$

where  $U$  and  $V$  are unitary matrices and  $\Sigma$  is a diagonal matrix with non-negative real numbers on the diagonal. The SVD is a generalization of the eigendecomposition of a positive semidefinite normal matrix to any  $m \times n$  matrix via an extension of the polar decomposition. It has many useful applications in signal processing and statistics. It can help us find the relevant states in large Hilbert spaces. Let's understand it using an example in following subsection;

### 1.7.1 Low-Rank Approximation

Low-rank approximation is a minimization problem, where the cost criterion is a measure of the fit between the given matrix (the data) and an approximating matrix

(the optimization variable), subject to a constraint that the approximating matrix has reduced rank. The best low-rank approximation can be found using the Singular Value Decomposition (SVD).

### 1.7.2 Image Compression using SVD

Implementation of SVD is done using Python. Please see the Appendix 3.1 for the python script. SVD can be used for image compression by representing the image as a matrix, where each entry corresponds to the pixel intensity. The SVD of this matrix is then computed. The singular values in the diagonal matrix  $\Sigma$  are sorted in descending order. Most of the singular values in  $\Sigma$  are close to zero and can be discarded without losing too much information. The remaining singular values represent the most significant features of the image.

The low-rank approximation of the image is then reconstructed using the reduced  $\Sigma$  along with  $U$  and  $V$  matrices. This results in a compressed version of the original image, as the reduced  $\Sigma$  takes much less space to store. The level of compression can be controlled by the number of singular values we choose to keep.

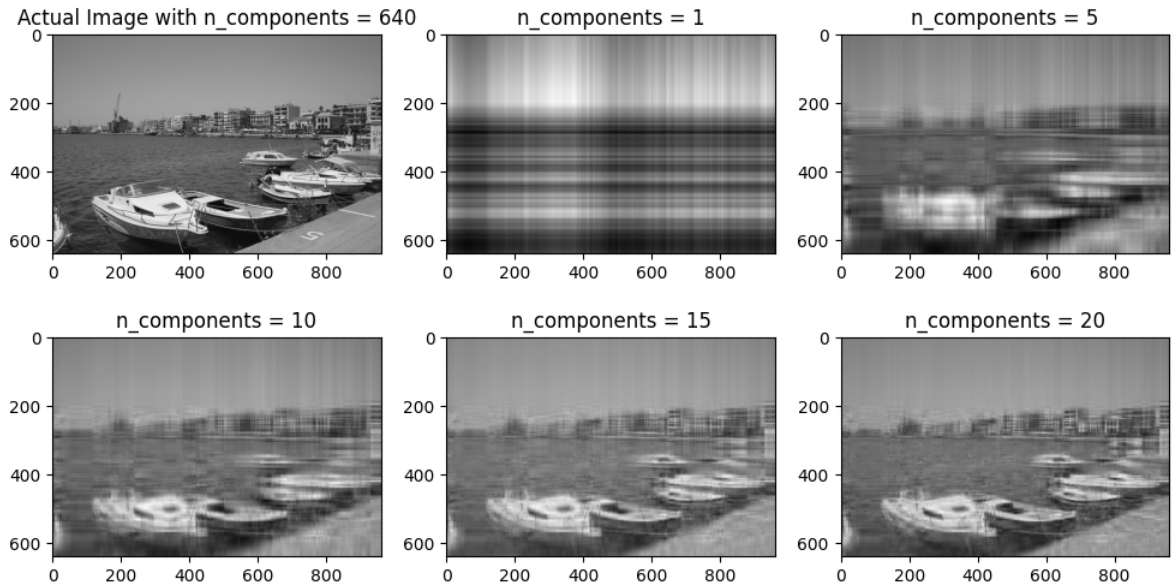


Figure 1.4: Image compression using SVD

In the figure above, the original image is represented as a matrix. The SVD of this matrix is computed and the singular values are sorted in descending order. The image is then reconstructed using a reduced number of singular values, resulting in a compressed version of the original image.

As you see in the following Figure most of the information is stored in the first few singular values.

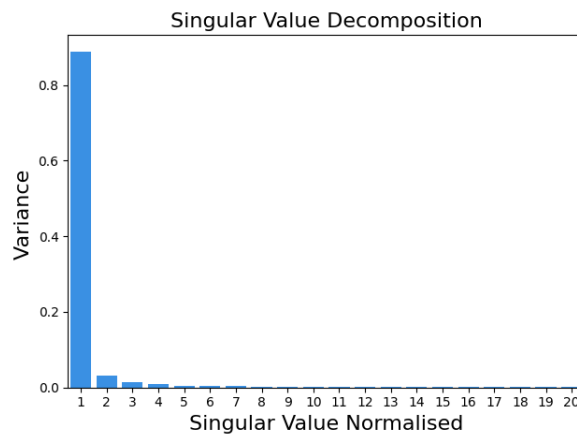


Figure 1.5: Singular values in descending order.



## Chapter 2

# Density Matrix Renormalization Group Algorithm (DMRG)

### 2.1 Introduction

The Density Matrix Renormalization Group (DMRG) algorithm is a tool used to derive a variational approximation for the ground states and low-lying excited states. It has been further adapted for use with finite temperature and dynamic properties.<sup>[7]</sup> There are two main types of this algorithm, as shown in Figure 2.1.

The finite-size algorithm is the most frequently used variant, where a matrix-product state (MPS) wavefunction on a finite-size lattice (characterized by a unique set of matrices  $A_n^{s_n}$  for each lattice site  $n = 1, 2, 3 \dots L$ , where  $|s_n\rangle$  is a  $d$ -dimensional basis for the local Hilbert space at site  $n$ ) is progressively refined until convergence.

In the infinite-size algorithm, the lattice expands by one or more sites at each iteration and eventually yields a wavefunction that exhibits translational invariance <sup>[7]</sup>.

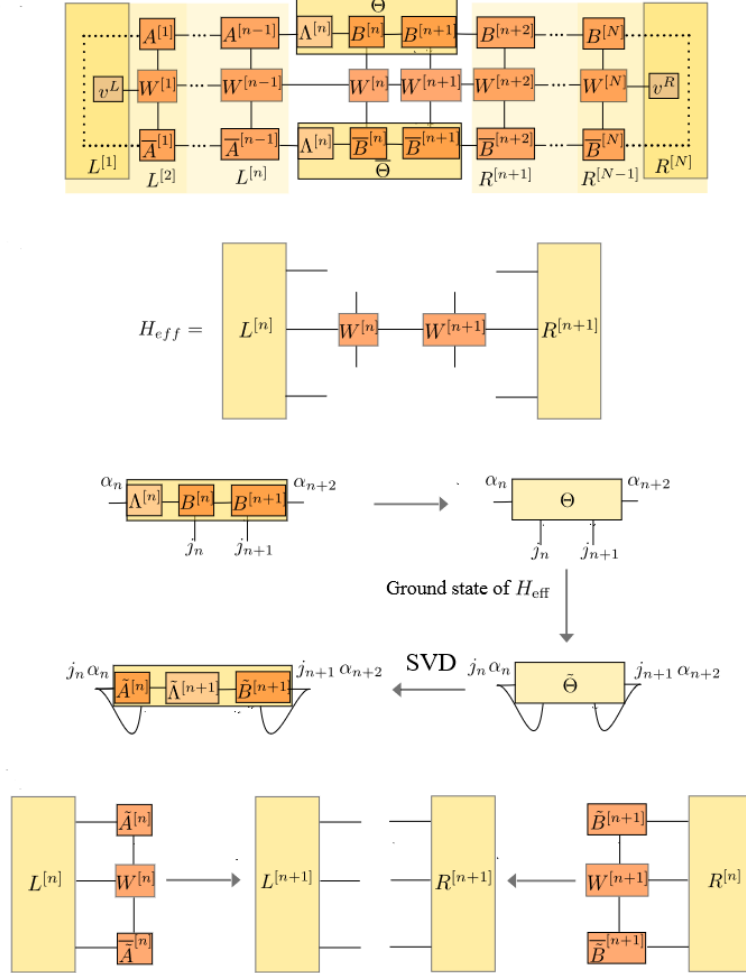


Figure 2.1: Step-by-step graphical representation of the DMRG algorithm. Structure of figure adopted from [8].

## 2.2 DMRG in the MPS formulation

The Density Matrix Renormalization Group (DMRG) algorithm, first introduced by Steven White in 1992 [9], was not originally designed within the Matrix Product States (MPS) framework. However, it has since been recognized as a powerful tool for identifying ground states in one-dimensional systems. The application of Matrix Product States offer a clear and efficient way to depict the DMRG algorithm.

## 2.3 iDMRG

The infinite-size Density Matrix Renormalization Group (iDMRG) algorithm is an extension of the DMRG algorithm that allows for the study of infinite systems. It was first introduced by McCulloch in 2008 [7].

The Density-Matrix Renormalization-Group (DMRG) algorithm has been widely used in various fields such as condensed matter physics, quantum chemistry, nuclear physics, and quantum information science. It provides a variational approximation for ground states and low-lying excited states. The algorithm comes in two forms: the finite-size algorithm and the infinite-size algorithm. The finite-size algorithm refines a matrix-product state (MPS) wavefunction on a finite-size lattice until convergence. The infinite-size algorithm expands the lattice by one or more sites each iteration, resulting in a translationally invariant wavefunction. This approach is useful for studying quantities in the thermodynamic limit, without the influence of boundary effects.

## 2.4 DMRG Algorithm

The following are the steps to implement DMRG algorithm:

1. Initialization:

- Obtain the wavefunction for a two-site lattice  $|\Psi_0\rangle = A_0^{s'_0} \Lambda_0 B_0^{s_0}$  and a four-site lattice  $|\Psi_1\rangle = A_0^{s'_0} A_1^{s'_1} \Lambda_1 B_1^{s_1} B_0^{s_0}$ .
- Set  $n = 1$  for the start of iterations.

2. Rotate the center matrix of  $|\Psi_n\rangle$  one step to the left, to obtain  $\dots \Lambda_n^L B_{n+1}^{s'_{n+1}} B_n^{s_n} \dots$

3. Rotate the center matrix of  $|\Psi_n\rangle$  one step to the right, to obtain  $\dots A_n^{s'_n} A_{n+1}^{s'_{n+1}} \Lambda_n^R \dots$

4. New wavefunction: The trial wavefunction for a lattice with size increased by two sites is given by  $|\Psi_{n+1}^{\text{trial}}\rangle = \dots A_{n+1}^{s'_{n+1}} \Lambda_n^R \Lambda_{n-1}^{-1} \Lambda_n^L B_{n+1}^{s_{n+1}} \dots$
5. Eigensolver: Use  $|\Psi_{n+1}^{\text{trial}}\rangle$  as the initial guess vector for an eigensolver, updating the matrices  $A_{n+1}^{s'_{n+1}} \Lambda_{n+1} B_{n+1}^{s_{n+1}}$  to obtain the final  $|\Psi_{n+1}\rangle$ .
6. Truncation: Truncate the dimension of  $\Lambda_{n+1}$  as desired, using eg. a singular value decomposition or eigenvalue decomposition, and normalize.
7. Stopping criteria: If  $\Lambda_{n+1}$  is sufficiently close to  $\Lambda_n^{L,R}$ , then the fixed point has been reached. Otherwise increase  $n \leftarrow n + 1$  and return to step 2.

# Chapter 3

## Transverse Field Ising Model (TFIM)

The Transverse Field Ising Model (TFIM) [10] is a model of spin-1/2 particles, defined by the following Hamiltonian:

$$H = -J \sum_{\langle i,j \rangle} \sigma_i^x \sigma_j^x - g \sum_i \sigma_i^z \quad (3.1)$$

This model includes nearest neighbor interactions based on the alignment of spin projections along the z-axis, and an external magnetic field perpendicular to the z-axis, which creates an energy preference for one x-axis spin direction over the other. The 1D model has two phases, depending on the ground state.

### 3.0.1 Ordered Phase

When  $|g| < 1$ , the system is in the ordered phase. In this phase, the ground state breaks the spin-flip symmetry, resulting in a two-fold degeneracy. The phase shows ferromagnetic ordering for  $J > 0$ , while for  $J < 0$ , antiferromagnetic ordering is observed.

$$|\psi\rangle_{GS} \rightarrow |\uparrow\uparrow\uparrow \dots| \downarrow\downarrow\downarrow \dots\rangle \quad (3.2)$$

This phase has a gapped characteristic, meaning that the lowest energy excited state(s) have an energy level that is a nonzero amount higher than the ground state energy, even in the thermodynamic limit. Specifically, this energy gap equals  $2|J|(1 - |g|)$ .

### 3.0.2 Disordered Phase

Conversely, when  $|g| > 1$ , the system is in the disordered phase. In this phase, the ground state preserves the spin-flip symmetry and is nondegenerate. As  $g \rightarrow \infty$ :

$$|\psi\rangle_{GS} \rightarrow |\rightarrow\rightarrow\rightarrow\rightarrow\dots\rangle \quad (3.3)$$

indicating spins aligned in the x-axis direction on each site. Like the ordered phase, this phase also has a gapped characteristic. The energy gap is given by  $2|J|(1 - |g|)$ .

### 3.0.3 Gapless Phase

When  $|g| = 1$ , the system undergoes a quantum phase transition. At this critical value of  $g$ , the system shows gapless excitations.

## 3.1 Results

We calculate various ground state properties of the TFIM for different values of the transverse field strength  $g$ . These properties include magnetization along the  $x$  and  $Z$  directions, energy per site, correlation functions between spins at different lattice sites, and the maximum bond dimension ( $\chi$ ) reached during the iterative Density Matrix Renormalization Group (iDMRG) optimization.

### 3.1.1 Correlation Length

The spin-spin correlation function  $\langle \sigma_{r_i}^z \sigma_j^z \rangle$  is calculated from the wavefunction  $|\psi\rangle$  obtained from iDMRG sweeps at different values of magnetic field  $g$ . The maximum correlation length obtained for  $i = L/4$  and  $j = 3L/4$  has been plotted against the magnetic field  $g$  in Figure 3.1.

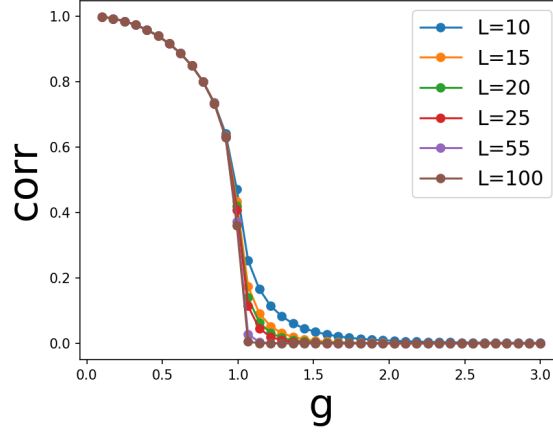


Figure 3.1: Correlation length vs  $g$  for various lattice sizes

### 3.1.2 Magnetisation in x-axis

The site expectation value for  $\sigma^x$  operator was calculated from the wavefunction  $|\psi\rangle$  obtained from iDMRG sweeps at different values of magnetic field  $g$ . The plot of  $\langle \sigma^x \rangle$  vs magnetic field  $g$  is given in Figure 3.2

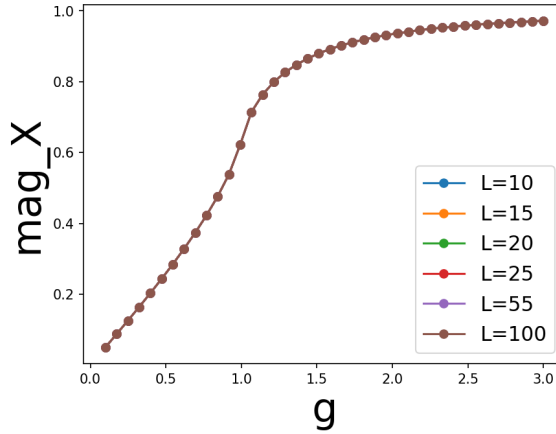


Figure 3.2:  $\langle \sigma^x \rangle$  vs  $g$  for various lattice sizes.

### 3.1.3 Magnetisation in z-axis

The expectation value of the  $\sigma^z$  operator was obtained similarly. The plot of  $\langle \sigma^z \rangle$  vs magnetic field  $g$  is given in fig.4.3. A quantum phase transition at  $|g| = 1$  is

observed from the plot. The system is in the ferromagnetic phase for  $g < J$ . In this phase, the system spontaneously breaks the symmetry in the thermodynamic limit, with two ground states  $|Z \approx \pm 1\rangle$ . In finite systems, there is a small splitting into the symmetric and anti-symmetric superpositions  $|Z \approx 1\rangle \pm |Z \approx -1\rangle$ , so that the true finite-L ground state has  $\langle Z \rangle = 0$ .

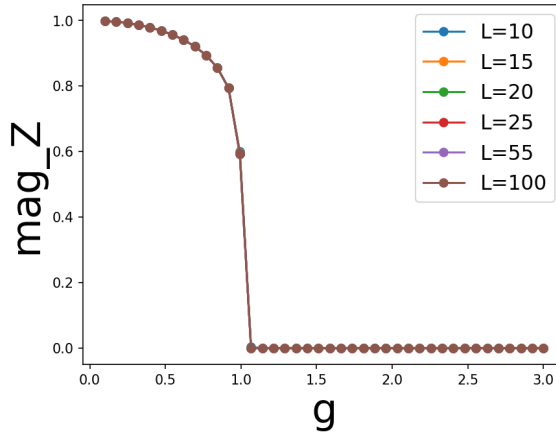


Figure 3.3:  $\langle \sigma^z \rangle$  vs  $g$  for various lattice sizes.

### 3.1.4 Max Bond Dimension $\chi$

During the iterative Density Matrix Renormalization Group (iDMRG) optimization, the maximum bond dimension ( $\chi$ ) serves as a crucial parameter reflecting the complexity of the wavefunction representation. The bond dimension determines the parameters required to describe the entanglement structure between adjacent lattice sites within the system. Please see Figure 3.4.



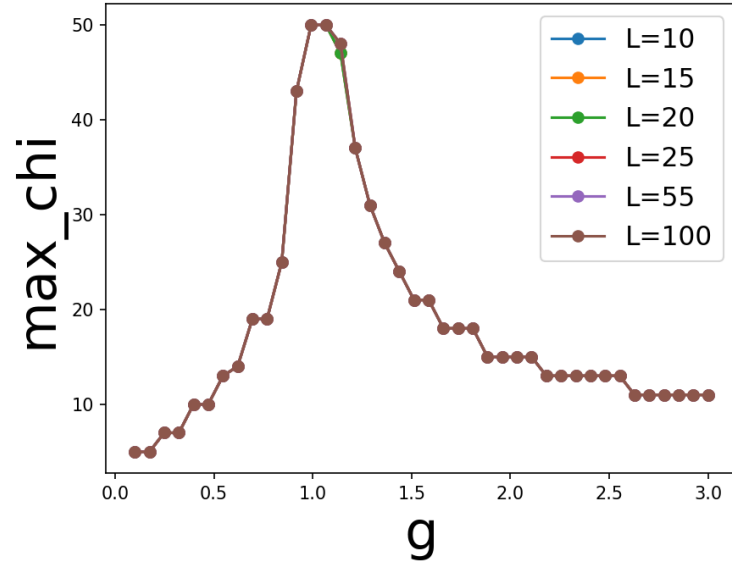


Figure 3.4: Max bond dimension vs  $g$  for various lattice sizes.

It is observed that the  $\chi_{max}$  peaks around  $|g| = 1$ .

This is because as the system approaches the critical point, the entanglement entropy increases, necessitating a larger bond dimension to capture the entanglement within the ground state wavefunction accurately.

# Appendix A

## 3.1 Singular Value Decomposition (SVD)

```
import requests

import cv2

import numpy as np

import matplotlib.pyplot as plt

url='https://cdn.pixabay.com/photo/2013/02/01/18/14/url-77169_960_720.jpg'
response = requests.get(url, stream=True)

with open('image.png', 'wb') as f:
    f.write(response.content)

img = cv2.imread('image.png')
gray_image = cv2.cvtColor(img, cv2.COLOR_BGR2GRAY)
u, s, v = np.linalg.svd(gray_image, full_matrices=False)
print(f'u.shape:{u.shape},s.shape:{s.shape},v.shape:{v.shape}')

import seaborn as sns
```

---

```
var_explained = np.round(s**2/np.sum(s**2), decimals=6)
print(f'variance Explained by Top 20 singular values:\n{var_explained[0:20]}')

sns.barplot(x=list(range(1, 21)), y=var_explained[0:20], color="dodgerblue")

plt.title('Singular Value Decomposition', fontsize=16)
plt.xlabel('Singular Value Normalised', fontsize=16)
plt.ylabel('Variance ', fontsize=16)
plt.tight_layout()
plt.show()

comps = [640, 1, 5, 10, 15, 20]
plt.figure(figsize=(12, 6))

for i in range(len(comps)):
    low_rank = u[:, :comps[i]] @ np.diag(s[:comps[i]]) @ v[:, comps[i], :]

    if(i == 0):
        plt.subplot(2, 3, i+1),
        plt.imshow(low_rank, cmap='gray'),
        plt.title(f'Actual Image with n_components = {comps[i]}')

    else:
        plt.subplot(2, 3, i+1),
        plt.imshow(low_rank, cmap='gray'),
        plt.title(f'n_components = {comps[i]}')
```

```
from tenpy.linalg import np_conserved as npc
from tenpy.networks.mps import MPS

tensor = npc.Array.from_ndarray_trivial(np.random.rand(4, 4, 4), ['p', 'q', 'r'])
mps = MPS.from_Bflat([tensor])
U, S, VH = mps.svd()
reconstructed_tensor = U.scale_axis(S, 1).matmul(VH)
print(np.allclose(tensor.to_ndarray(), reconstructed_tensor.to_ndarray()))
```

# References

- [1] J Rodríguez-Laguna. Quantum wavefunction annealing of spin glasses on ladders. *Journal of Statistical Mechanics: Theory and Experiment*, 2007(05):P05008, may 2007.
- [2] Annika Völl and Stefan Wessel. Spin dynamics of the bilinear-biquadratic  $s = 1$  heisenberg model on the triangular lattice: A quantum monte carlo study. *Phys. Rev. B*, 91:165128, Apr 2015.
- [3] Max Haller, Patrick Malaise, and Fritz Schiltz. Matrix product states: A variational approach to strongly correlated systems. 25:51–61, 2021.
- [4] D. Perez-Garcia, F. Verstraete, M. M. Wolf, and J. I. Cirac. Matrix product state representations, 2007.
- [5] Román Orús. A practical introduction to tensor networks: Matrix product states and projected entangled pair states. *Annals of Physics*, 349:117–158, October 2014.
- [6] Johannes Hauschild and Frank Pollmann. Efficient numerical simulations with Tensor Networks: Tensor Network Python (TeNPy). *SciPost Phys. Lect. Notes*, page 5, 2018.
- [7] I. P. McCulloch. Infinite size density matrix renormalization group, revisited, 2008.
- [8] J. Hauschild and F. Pollmann. page 5, May 2018.
- [9] Steven R. White. Density-matrix algorithms for quantum renormalization groups. *Phys. Rev. B*, 48:10345–10356, Oct 1993.

- [10] Pierre Pfeuty. The one-dimensional ising model with a transverse field. *Annals of Physics*, 57(1):79–90, 1970.